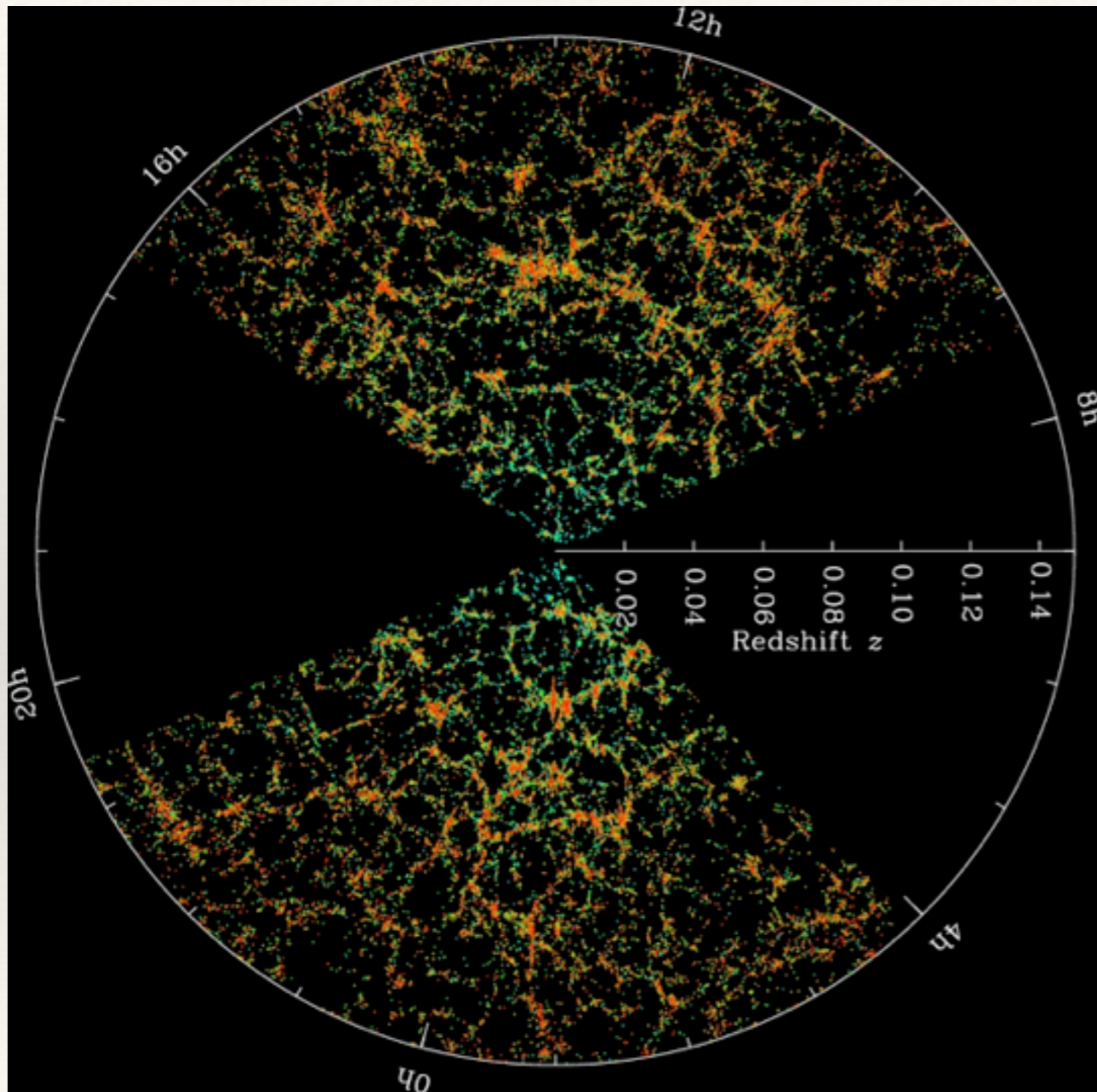

Pseudo-spectrum analysis
of galaxy-galaxy lensing

Chiaki Hikage
(Kavli IPMU)

Galaxy redshift surveys



SDSS Collaboration

Science goals

- Dark energy
- Dark matter
- Neutrino mass
- Primordial Non-Gaussianity

Galaxy redshift surveys

- CfA, LCRS, 2dF, SDSS, BOSS, WiggleZ, VVDS, Vipers, FastSound
- PFS, HETDEX, eBOSS, Euclid, WFIRST

Uncertainty of galaxy biasing

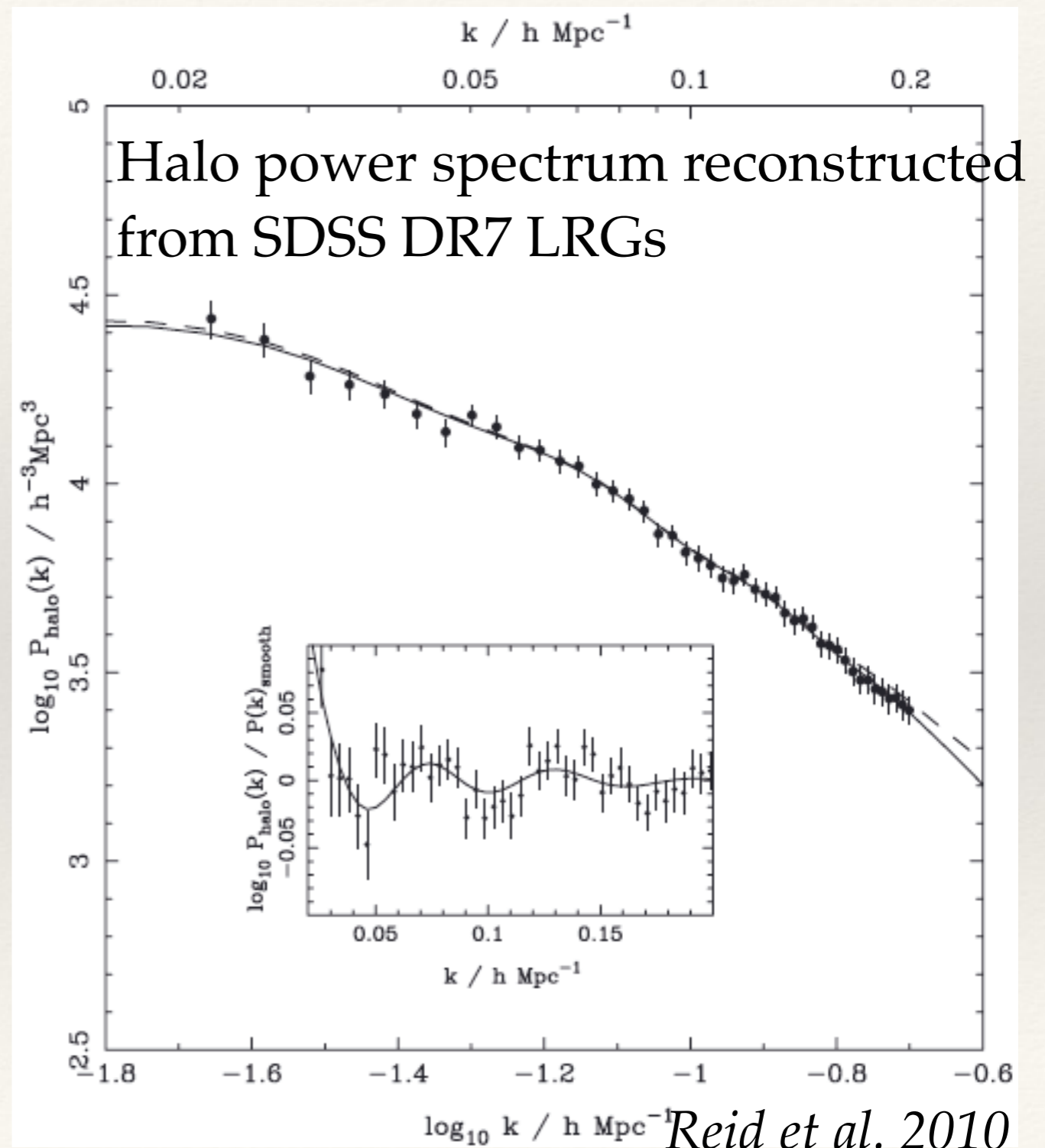
Relationship between galaxy number density field δ_g and mass density field δ_m

$$\delta_g(\mathbf{k}) = \mathbf{b}(\mathbf{k}) \delta_m(\mathbf{k})$$

galaxy power spectrum:

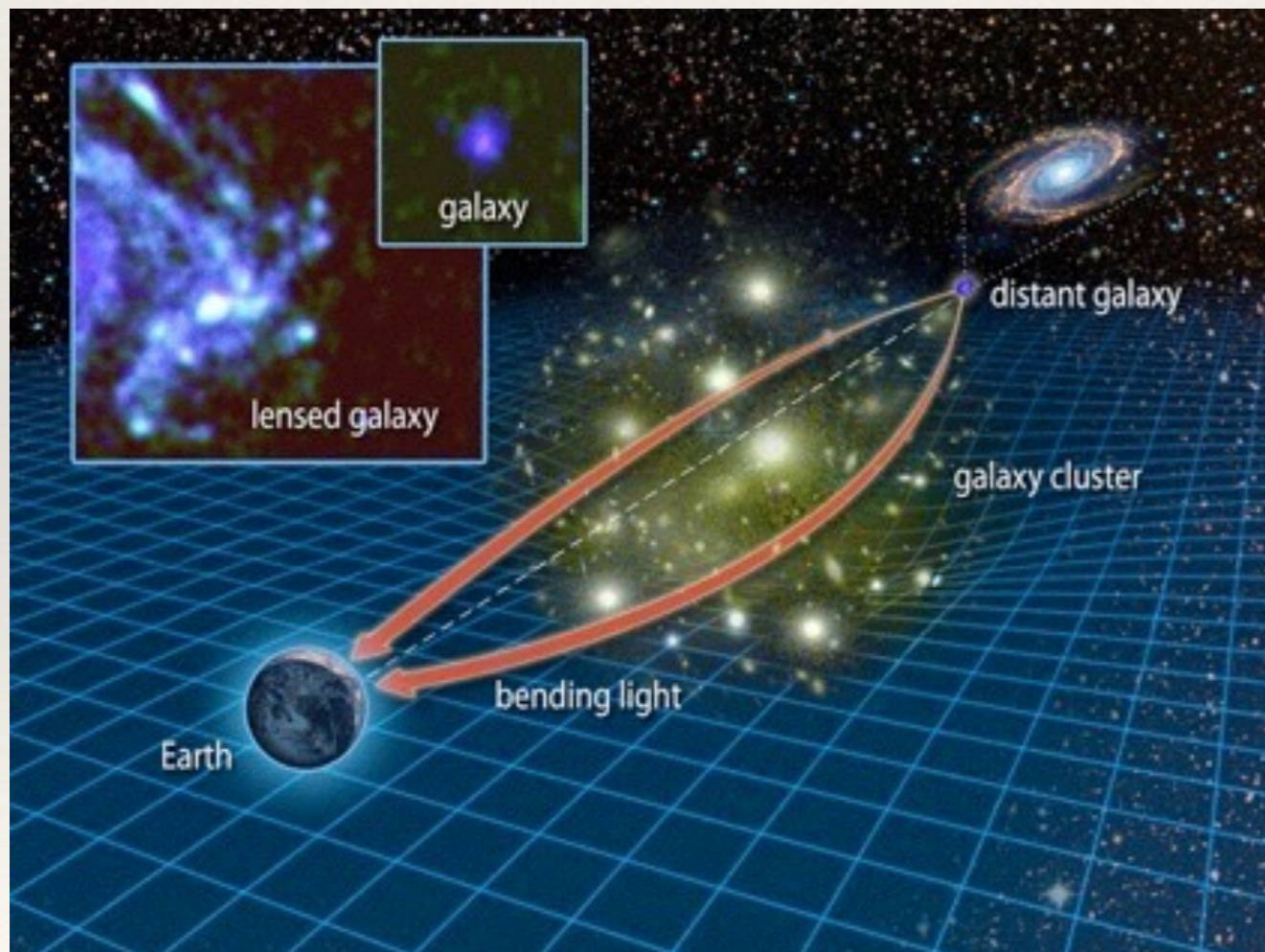
$$P_{gg}(\mathbf{k}) = \mathbf{b}^2(\mathbf{k}) P_{mm}(\mathbf{k})$$

galaxy biasing depends on scale, redshift, galaxy types, ..



galaxy-galaxy lensing

- ❖ Cross correlation between foreground galaxies and background galaxy image distortion



galaxy-DM cross spectrum

$$P_{gm}(k) = b(k)P_{mm}(k)$$

Combination of P_{gg} and P_{gm}
can reduce bias uncertainty

SUbaru Measurement of Images and REdshift

Joint Mission of Imaging and Redshift surveys using 8.2m Subaru Telescope

Hyper-Suprime Cam (HSC)

- 1300 deg² sky (overlap w/ ACT, BOSS)
- 30gals / arcmin², $z_{\text{mean}}=1$, $i \sim 26(5\sigma)$
- 1.5 deg FoV, grizy band, 0.16"pix,
- 2014-2018

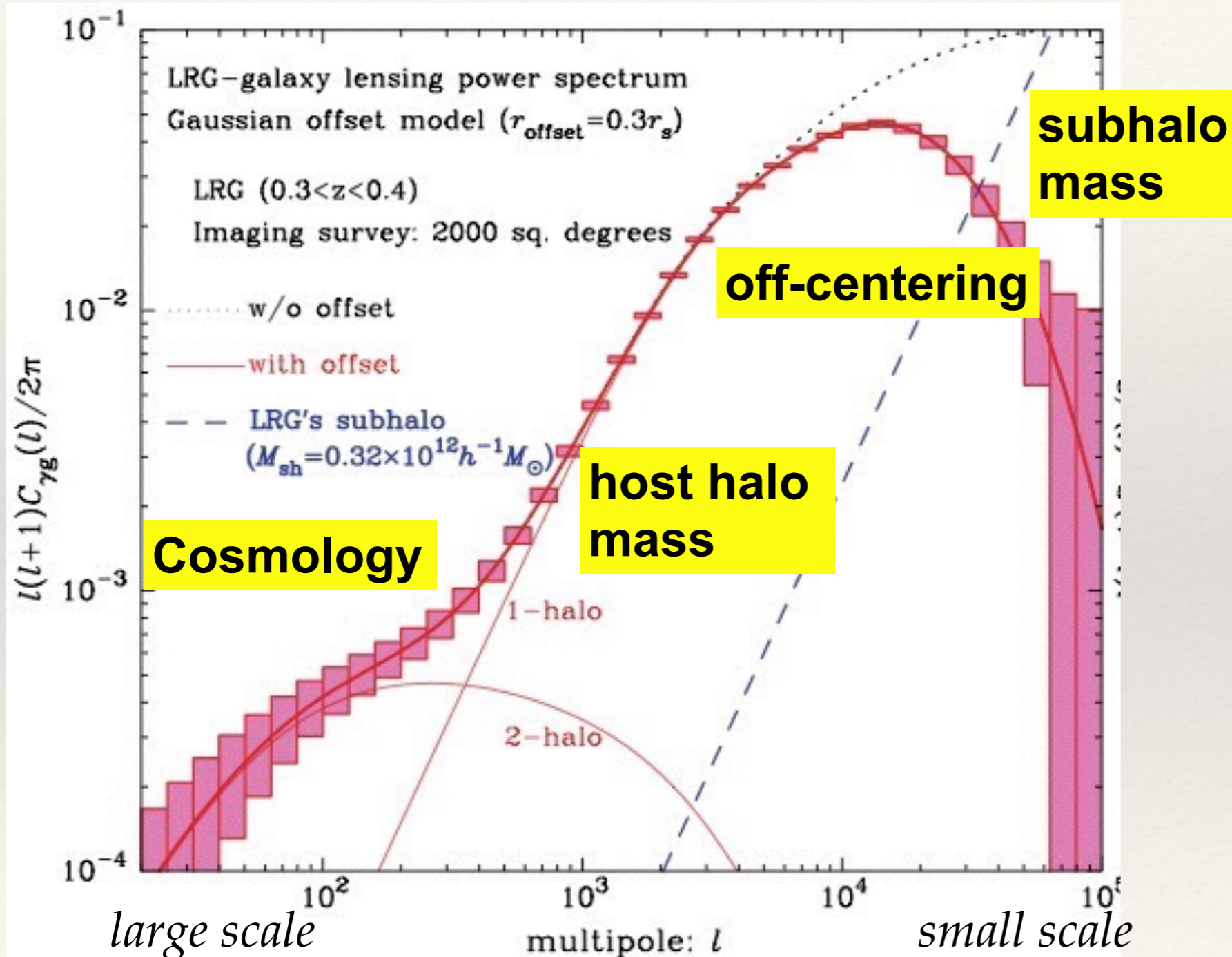
Prime Focus Spectrograph (PFS)

- 1300 deg² of sky (overlap w/ HSC)
- Redshift of LRGs + OII emitters at $0.8 < z < 2.4$ (9.3 Gpc/h³ comoving vol)
- 2400 fibers, 380~1300nm (R~3000)
- 2019-2023 (planned)



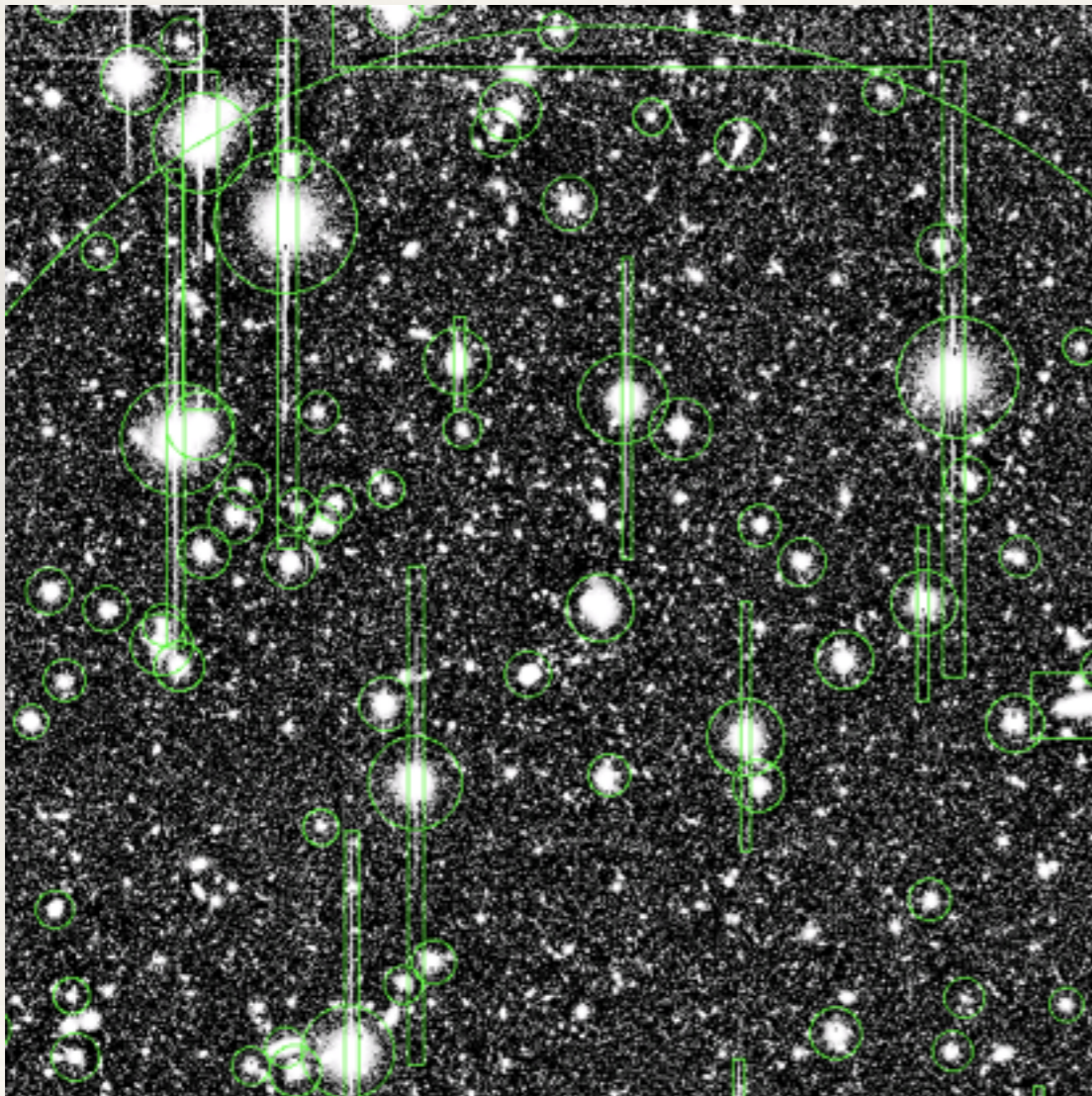
Mauna Kea, Hawaii,
4139m alt., 0.6-0.7" seeing

g-g lensing expected from HSC+LRG

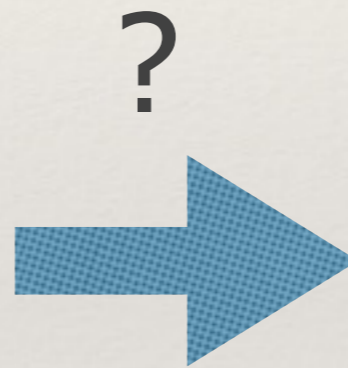


How can we measure lensing spectrum ?

20-30% of sky is masked by bright stars



Suprime Cam



lensing power spectrum

g-g lensing spectrum

Convolution of survey mask

obs mask (weight) true

$$\tilde{\gamma}_1(\mathbf{n}) \pm i\tilde{\gamma}_2(\mathbf{n}) = W(\mathbf{n})[\gamma_1(\mathbf{n}) \pm i\gamma_2(\mathbf{n})] \quad W(\mathbf{n}) : \text{mask field}$$

$$\tilde{E}_{\mathbf{k}} \pm i\tilde{B}_{\mathbf{k}} = \sum_{\mathbf{n}} [\tilde{\gamma}_1(\mathbf{n}) \pm i\tilde{\gamma}_2(\mathbf{n})] \exp(-i\mathbf{k} \cdot \mathbf{n} \pm 2\varphi_{\mathbf{k}})$$

$$= \sum_{\mathbf{k}'} [E_{\mathbf{k}'} \pm iB_{\mathbf{k}'}] W_{\mathbf{k}-\mathbf{k}'} \exp(\pm 2(\varphi_{\mathbf{k}'} - \varphi_{\mathbf{k}}))$$

E-mode and B-mode power spectrum

$$\begin{pmatrix} \tilde{C}_{\mathbf{k}}^{EE} \\ \tilde{C}_{\mathbf{k}}^{BB} \end{pmatrix} = \sum_{\mathbf{k}'} W_{\mathbf{k}-\mathbf{k}'} \begin{pmatrix} \cos^2 2\varphi_{\mathbf{k}'\mathbf{k}} & \sin^2 2\varphi_{\mathbf{k}'\mathbf{k}} \\ \sin^2 2\varphi_{\mathbf{k}'\mathbf{k}} & \cos^2 2\varphi_{\mathbf{k}'\mathbf{k}} \end{pmatrix} \begin{pmatrix} C_{\mathbf{k}'}^{EE} \\ C_{\mathbf{k}'}^{BB} \end{pmatrix} + \begin{pmatrix} \tilde{N}_{\mathbf{k}} \\ \tilde{N}_{\mathbf{k}} \end{pmatrix}$$

E-B mode mixing due to mask

$$\cos \varphi_{\mathbf{k}'\mathbf{k}} = \mathbf{k}' \cdot \mathbf{k} / k' k$$

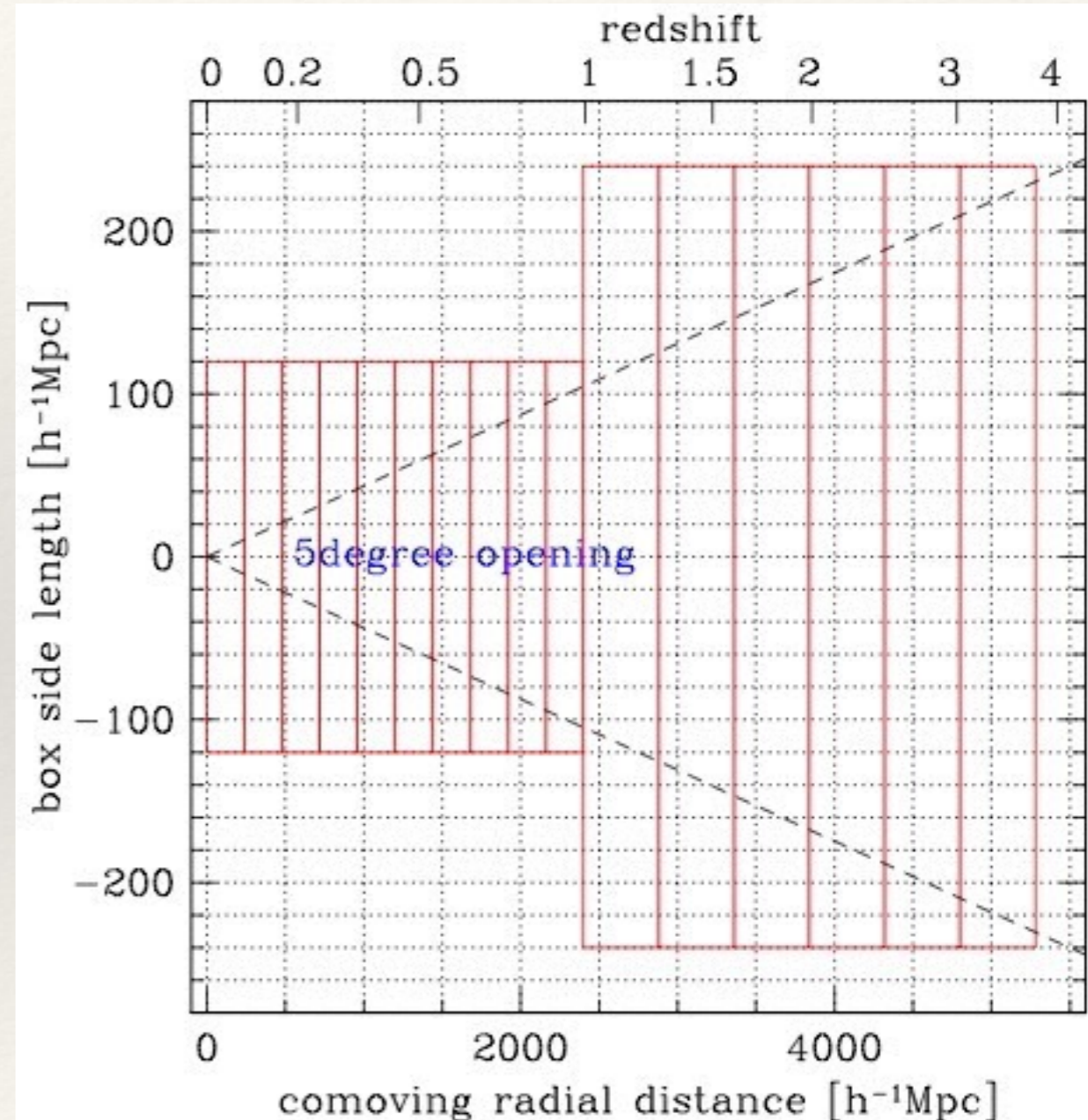
Reconstruction of power spectrum

$$\overset{\text{true}}{C_b} = \overset{\text{mask}}{M_{bb'}^{-1}} \sum_{k \in k'_b} P_{b'k} (\overset{\text{obs}}{\tilde{C}_k} - \langle \tilde{N}_k \rangle_{\text{MC}}), \quad \text{noise}$$

- ⊕ Commonly used to reconstruct CMB temperature/polarization spectrum (e.g., Hivon et al. 2002)
 - ⊕ Analogy to CMB polarization (Q,U) \Leftrightarrow (γ_1, γ_2)
- ⊕ Noise spectrum is estimated by randomly rotating shapes

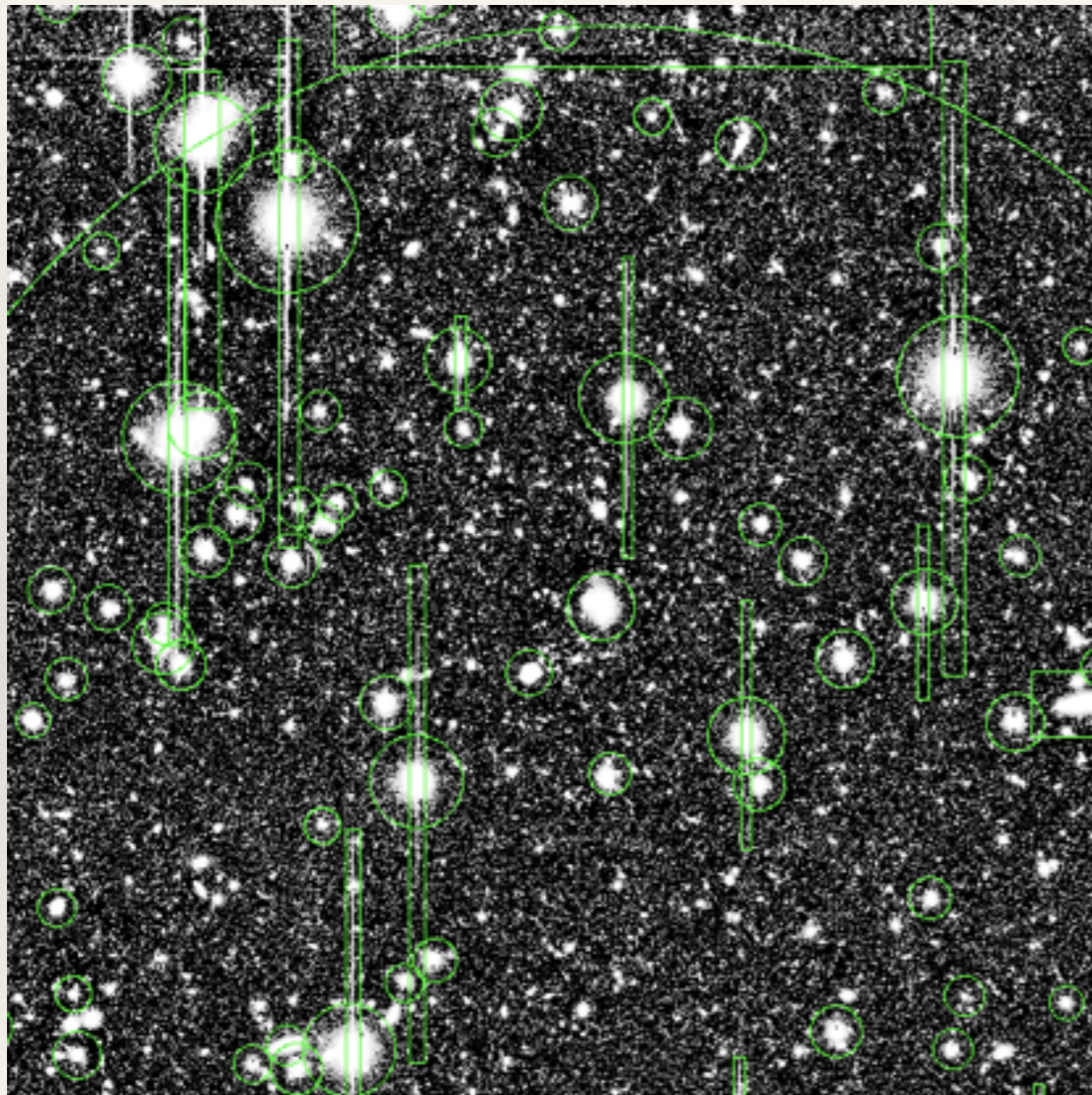
Ray-Tracing Simulations (Sato et al. 2009)

- ❖ N-body simulations
 - ❖ Gadget 2 at $z_{\text{init}}=50$
 - ❖ 200 realizations with $L_{\text{box}}=240$ and $480\text{Mpc}/h$
 - ❖ ΛCDM based on WMAP 3
- ❖ Ray-Tracing simulations
 - ❖ $5^\circ \times 5^\circ$, 2048^2 grids (grid size: $0.15'$)
 - ❖ Multiple lens plane algorithm (Jain et al. 2000)
 - ❖ Lens plane width $\Delta\chi=120\text{Mpc}/h$, $z=0 - 3.5$
 - ❖ 1000 realizations

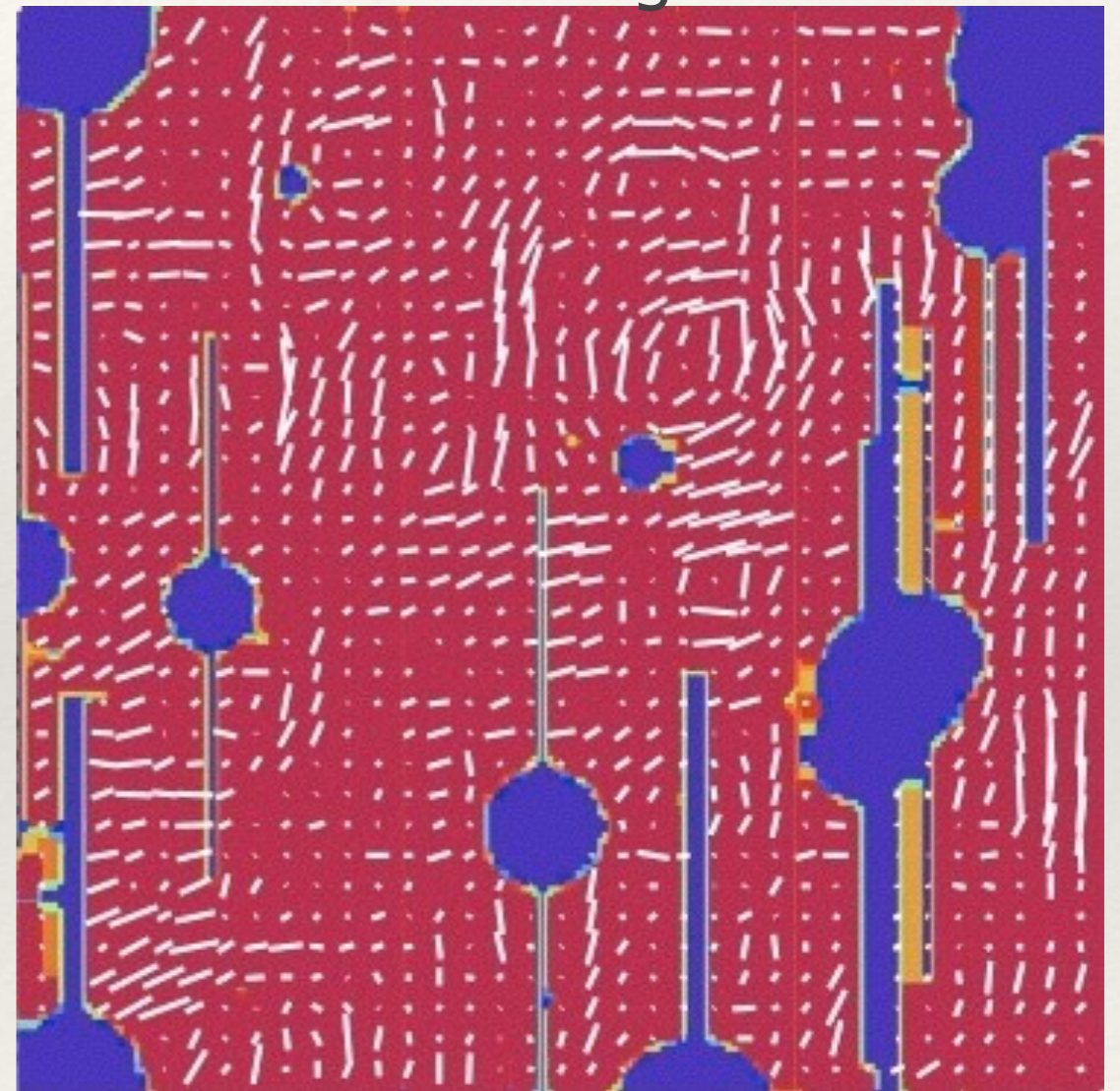


Mock star mask

side length: 20 arcmin



Suprime Cam

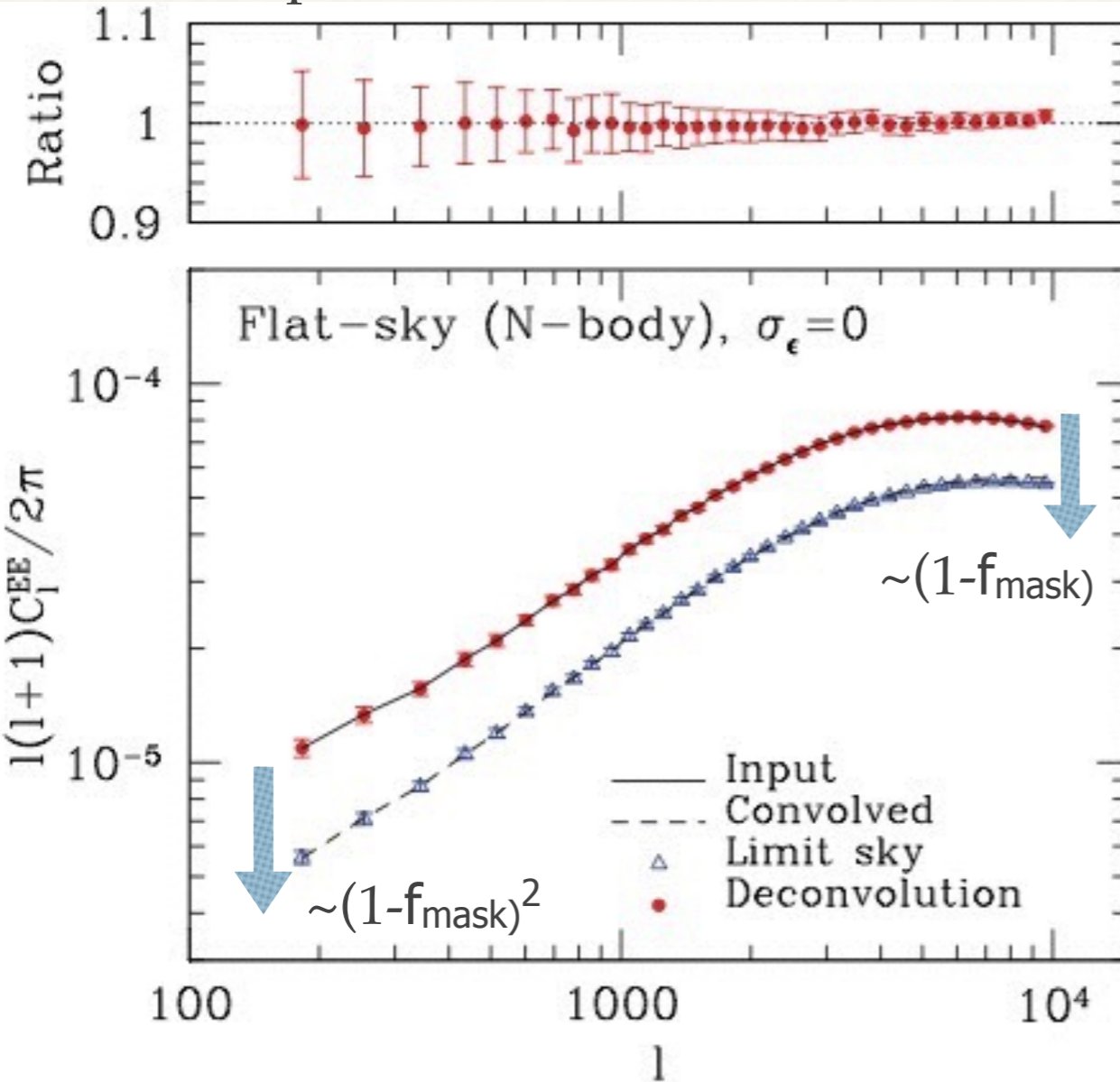


CH, Takada, Hamana, Spergel 2009

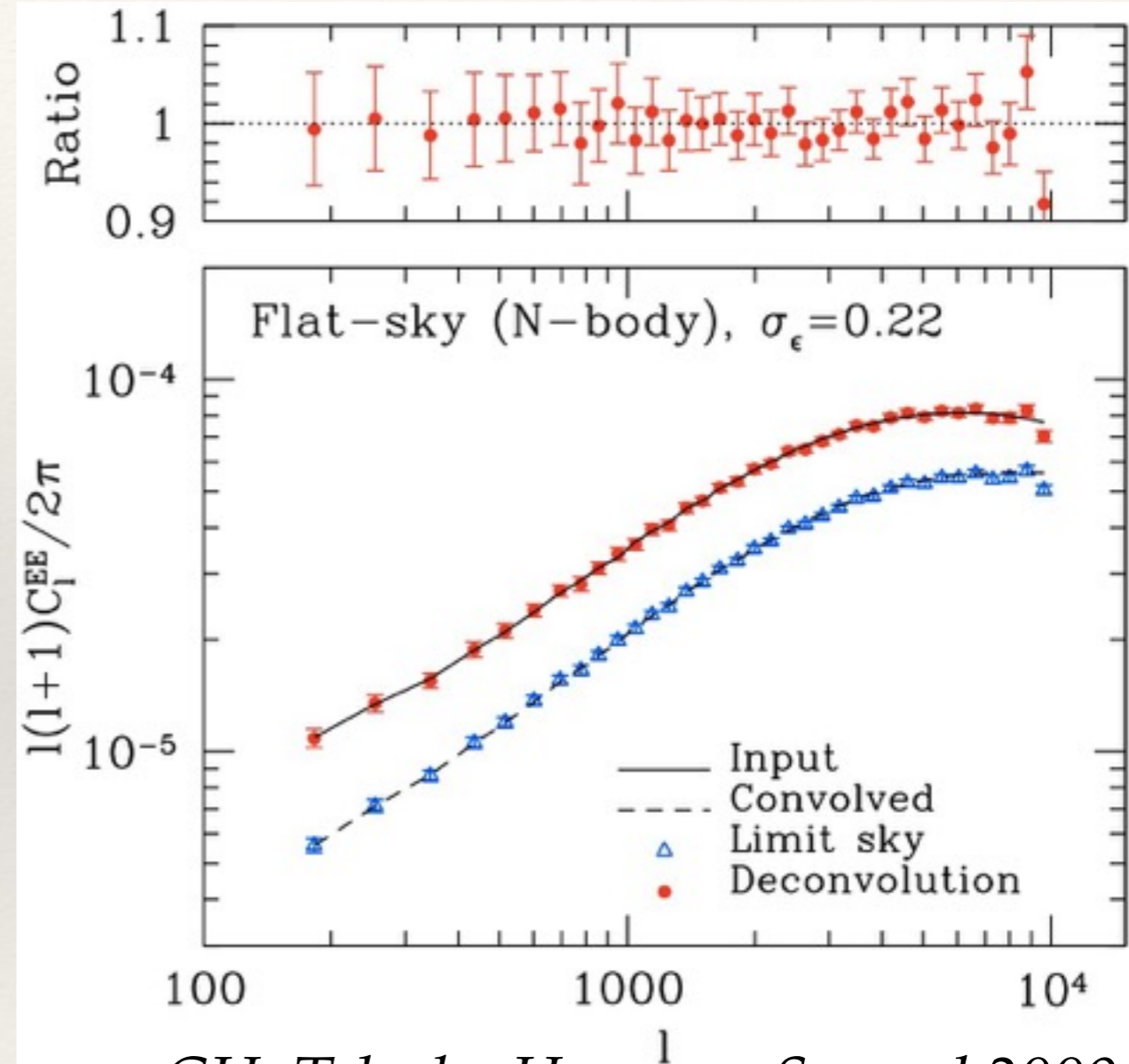
25% field is masked

Reconstruction of lensing power spectrum

w/o shape noise



w/ shape noise ($\sigma_{\text{noi}}=0.22$)

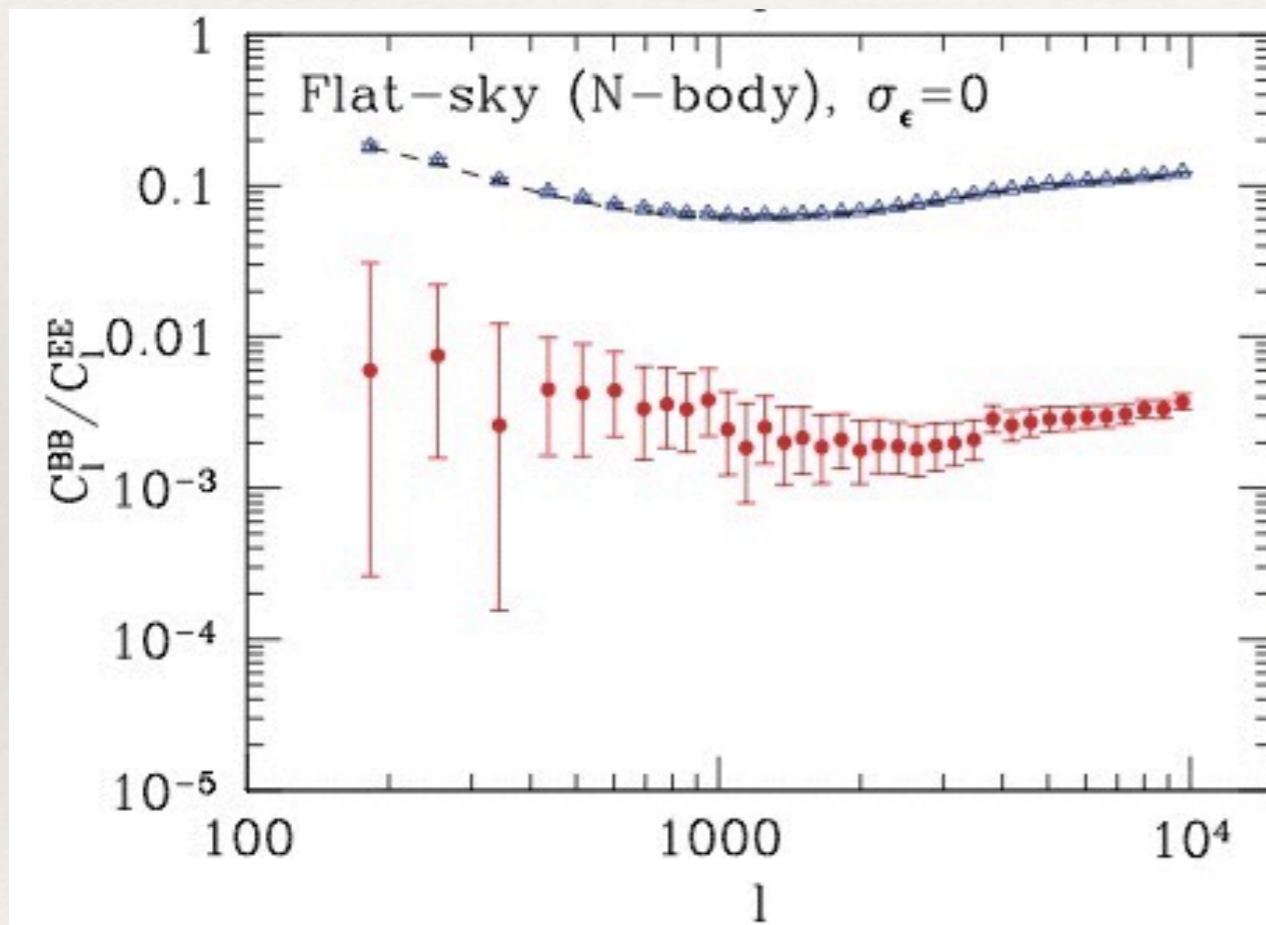


CH, Takada, Hamana, Spergel 2009

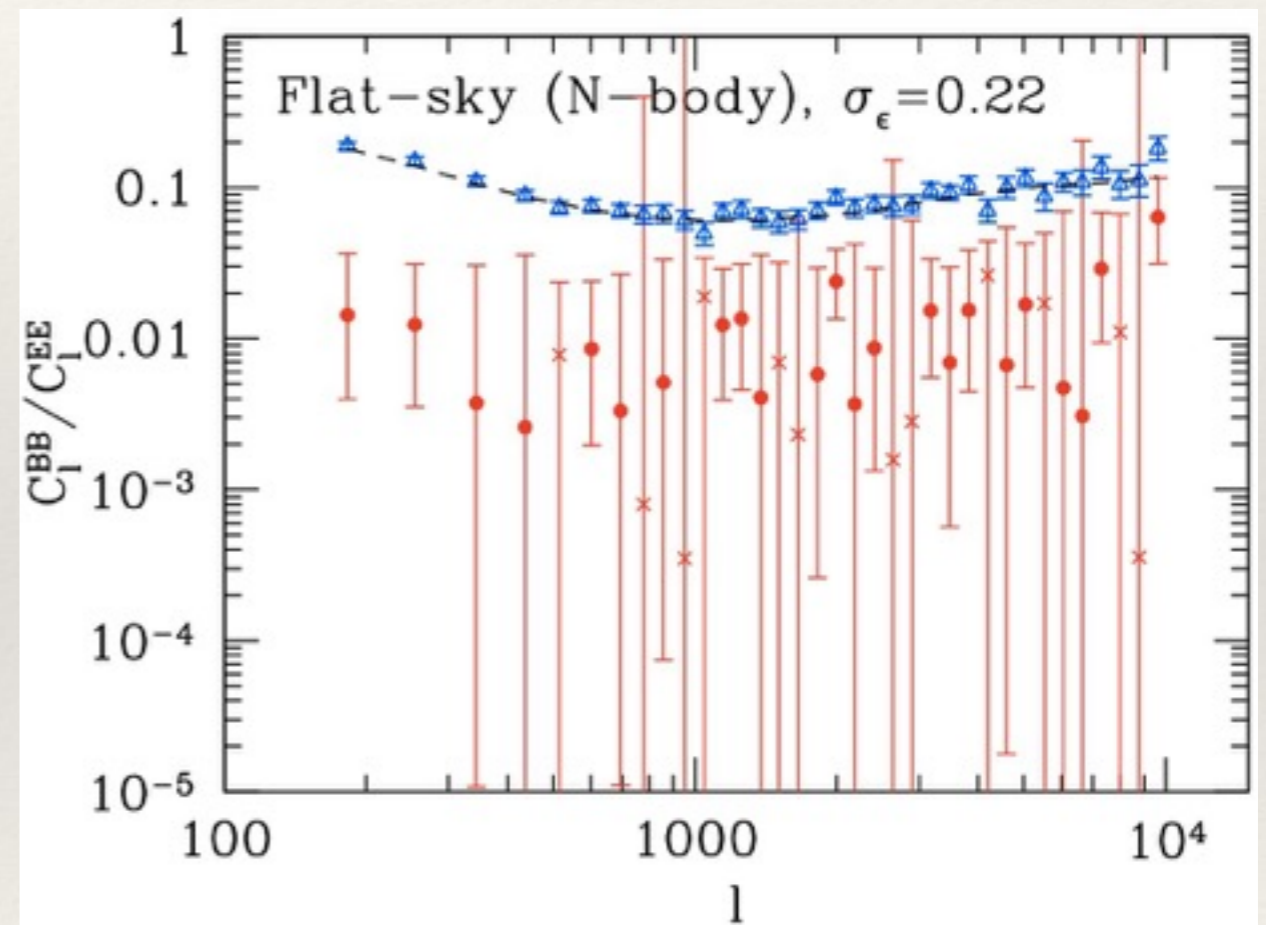
Input lensing power spectrum is successfully reconstructed

B-mode contamination

w/o shape noise



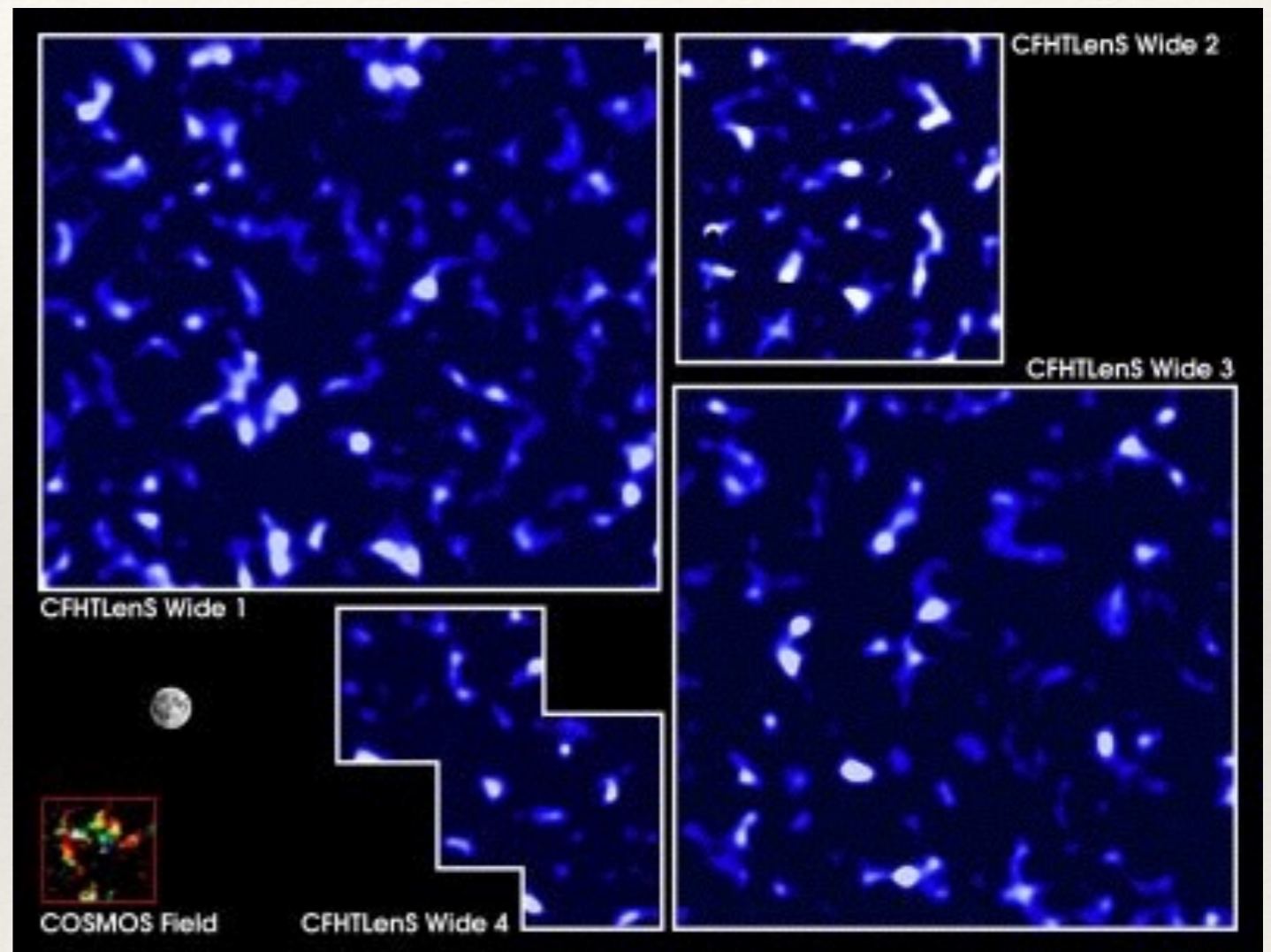
w/ shape noise



Residual B-mode is suppressed below a percent of E-mode

CFHTLenS public data

- ❖ $\Omega_{\text{sky}}=154 \text{ deg}^2$ for 4 CFHTLS fields (W1 – W4)
- ❖ $n_{\text{gal}}=17 \text{ arcmin}^2$, $z_{\text{mean}}=0.75$
- ❖ 5-year data taken in Hawaii
- ❖ Lensfit: Bayesian model fitting method of shape measurement
- ❖ Bayesian Photometric Redshift Code (BPZ)



Credit: Van Waerbeke, C. Heymans

CFHTLenS power spectrum



Preliminary results of CFHTLenS lensing power spectrum

Error: sample variance estimated from 4 CFHTLS fields

B-mode is consistent with zero up to $l < 4000$

pseudo-spectrum for galaxy-galaxy lensing

shear field

$$\tilde{\gamma}(\mathbf{n}) = W_{\gamma}(\mathbf{n})\gamma(\mathbf{n})$$

weight for shear field: source numbers, shape noise, intrinsic noise

2D galaxy number density field

$$\tilde{\delta}_g(\mathbf{n}) = W_g(\mathbf{n})\delta_g(\mathbf{n})$$

weight for density field: angular selection function, redshift failure, fiber collision

galaxy-galaxy lensing spectrum

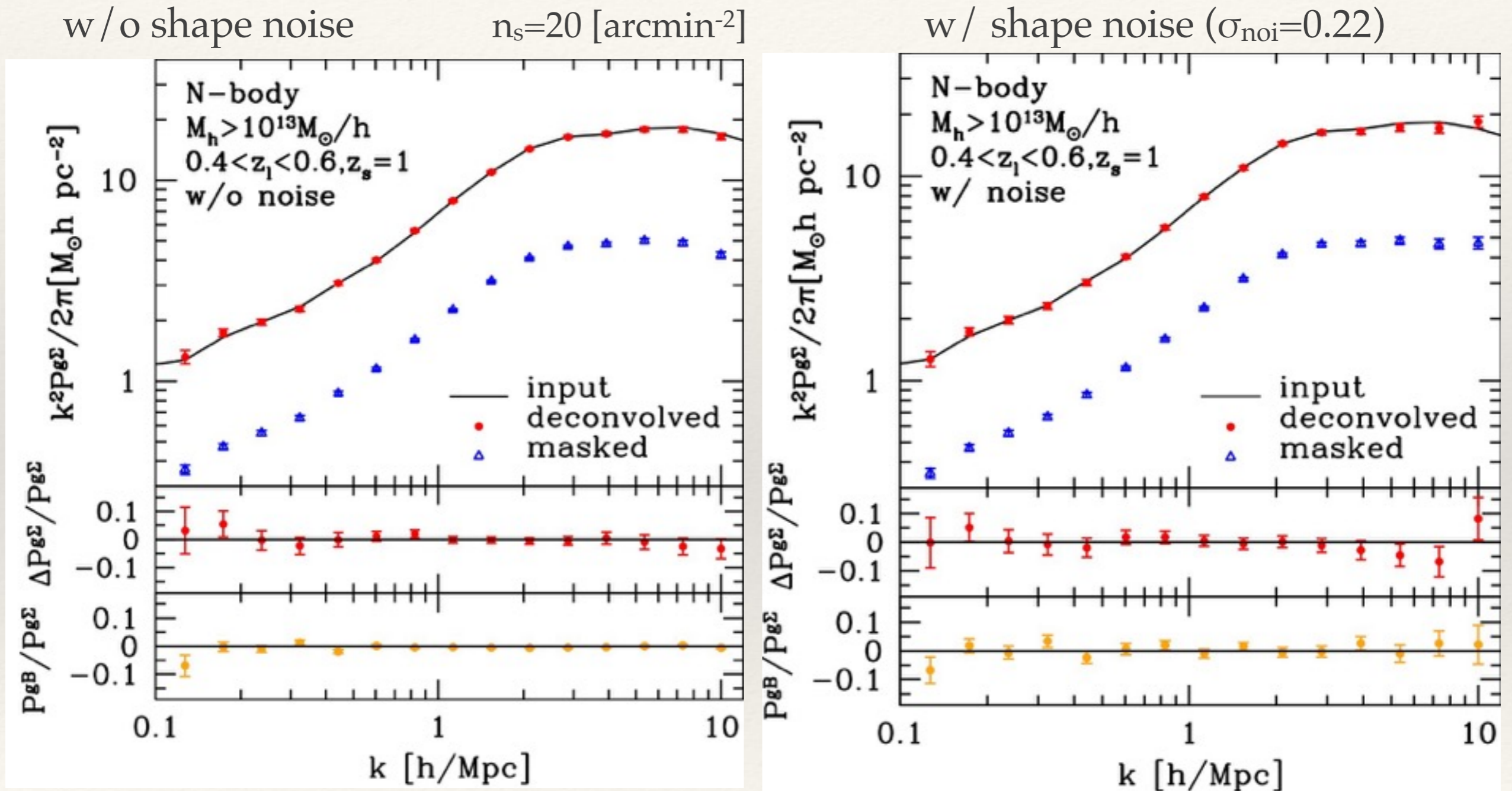
cross spectrum of the two weight fields

$$\tilde{C}_1^{\text{gE(B)}} = \frac{1}{L^2} \sum_{l'} C_{l'}^{\text{gE(B)}} \mathcal{W}_{1-l'}^{\text{g}\gamma} \cos(2\varphi_{ll'})$$

$$\langle W_1^g W_{l'}^{\gamma*} \rangle = L^2 \delta_{1-l'}^W \mathcal{W}_1^{\text{g}\gamma}$$

Pseudo-spectrum method can be applied for g-g lensing spectrum

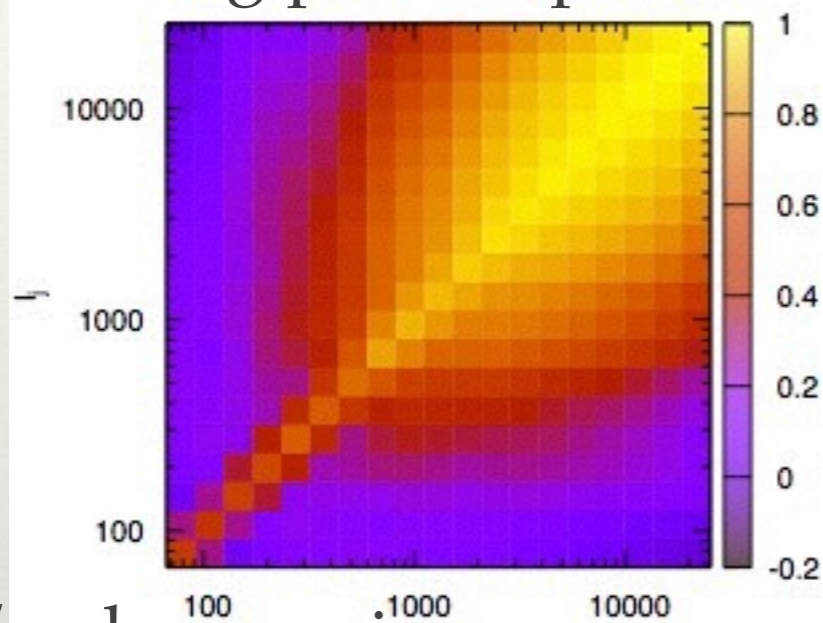
Reconstruction of galaxy (halo) lensing spectrum



Input halo lensing spectrum is successfully reconstructed

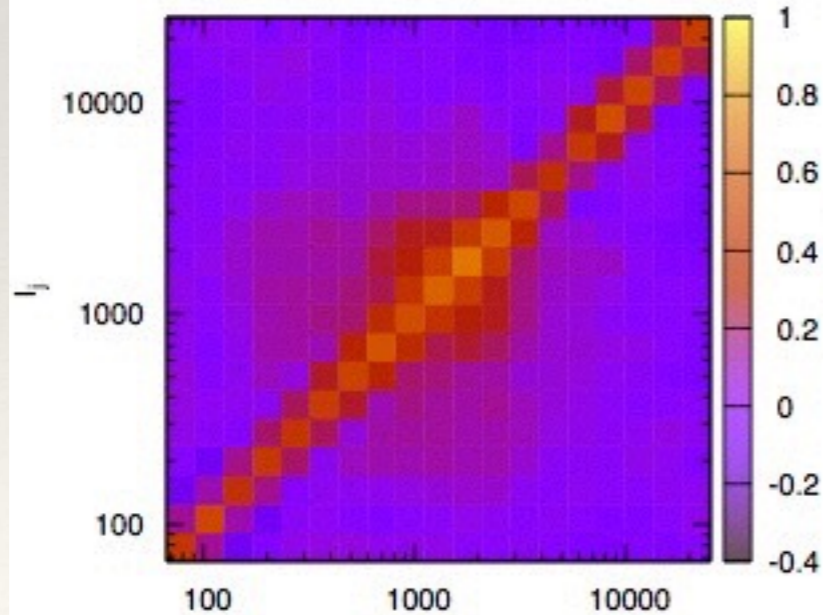
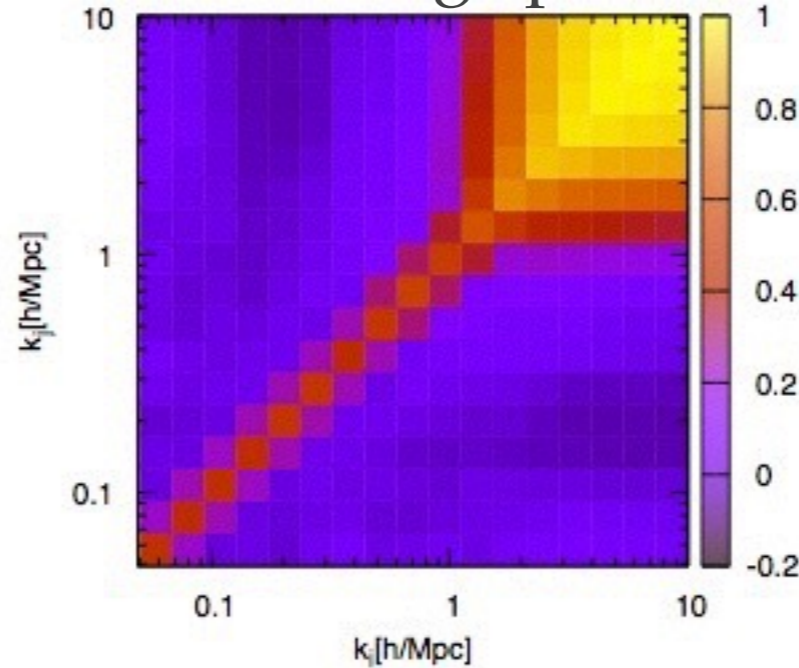
Covariance matrix

lensing power spectrum

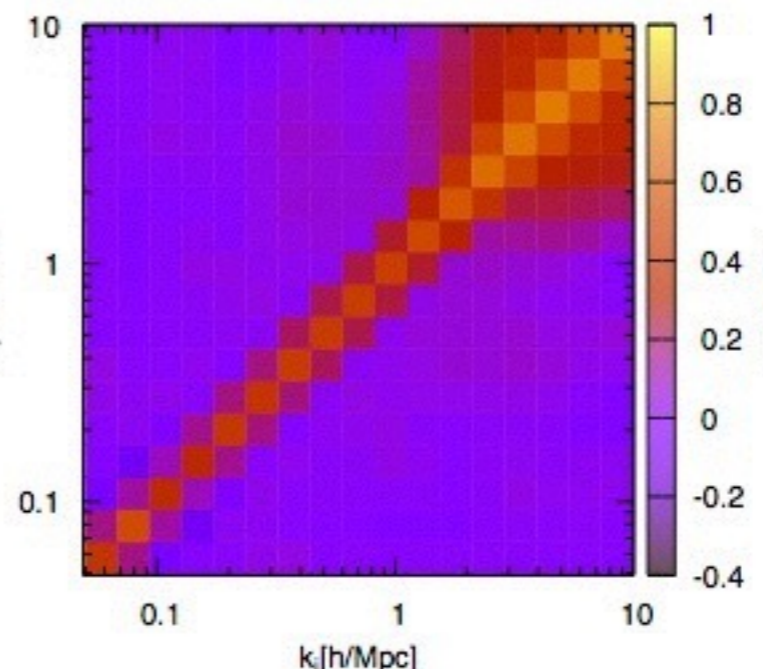


w/o shape noise

halo lensing spectrum



w/ shape noise ($\sigma_{\text{noi}}=0.22$)



source:

$$z_s=1$$

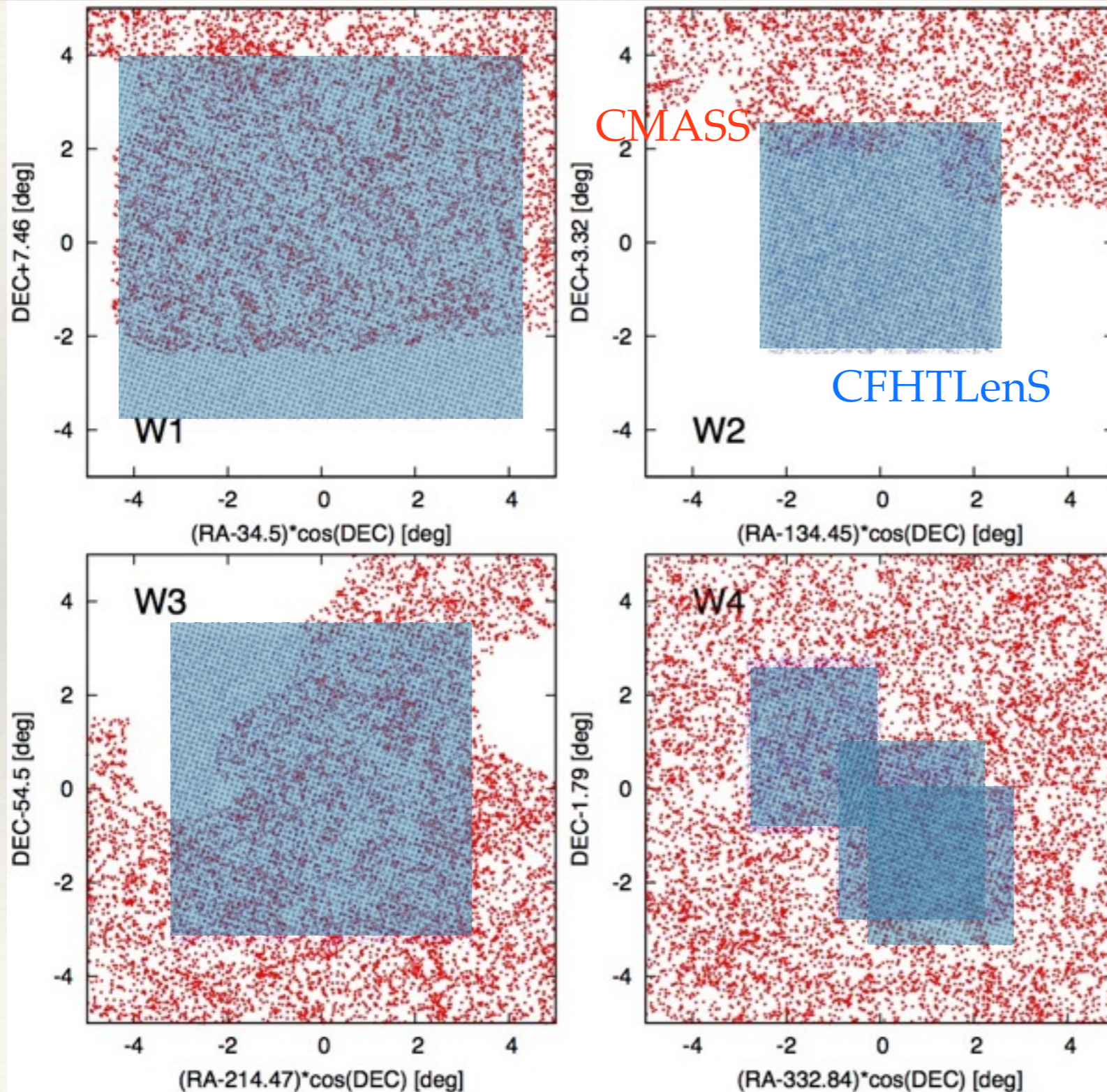
$$n_{\text{gal}}=20 \text{ arcmin}^{-2}$$

halo:

$$M_h > 10^{13} M_{\text{sun}} / h$$

$$0.4 < z < 0.6$$

CFHTLenS + SDSS



Overlapped area for
CMASS galaxies $\sim 100 \text{ deg}^2$

3 spectroscopic samples

- SDSS DR7 LRG

($0.16 < z < 0.33$) : $N_g = 445$

- BOSS LOWZ

($0.16 < z < 0.33$) : $N_g = 2396$

- BOSS CMASS

($0.47 < z < 0.59$) : $N_g = 5415$

observed g-g lensing spectrum



Preliminary results of g-g lensing

Residuals systematics of shape measurement is subtracted

Error includes Poisson error and sample variance estimated from 4 CFHTLS fields

We use source galaxies with $P(z_{\text{BPZ}} > z_{1,\text{max}}) > 0.84$

Halo model

$$P_{g\kappa} = P_{g\kappa}^{1h} + P_{g\kappa}^{2h}$$

1-halo term

HOD parameters

$$P_{g\kappa}^{1h}(k) = \int d\chi \left(\frac{W_g(z)W_\kappa(z)}{\chi^2(z)} \right) \int dM \frac{dn}{dM} \frac{M}{\bar{\rho}_m} \tilde{u}_{\text{NFW}}(k; M, z) [\langle N_{\text{cen}} \rangle + \langle N_{\text{sat}} \rangle \tilde{p}_{\text{sat}}(k; M)]$$

off-centering profile of satellites

$$\tilde{p}_{\text{sat}}(k; M) = \exp(-k^2 R_{\text{vir}}^2(M)/2)$$

2-halo term

$$P_{g\kappa}^{2h}(k) = \int d\chi \left(\frac{W_g(z)W_\kappa(z)}{\chi^2(z)} \right) \left[\int dM \frac{dn}{dM} (\langle N_{\text{cen}} \rangle + \langle N_{\text{sat}} \rangle \tilde{p}_{\text{sat}}(k; M)) P_{\text{hm}}(k, z; M) \right]$$

halo matter power spectrum

$$P_{\text{hm}}(k, z; M) = b(M, z) P_{\text{mm}}^{(\text{lin})}(k, z)$$

linear bias (Tinker et al. 2010)

Comparison with halo model: LRG

HOD for LRGs: Reid, Spergel 2009



Preliminary results of LRG-galaxy lensing

LRG lensing spectrum is consistent with halo model predictions

Summary

- ❖ We apply pseudo-spectrum analysis to measure lensing power spectrum and galaxy-galaxy lensing
- ❖ We find that observed g-g lensing spectrum using CFHTLenS and SDSS LRG, BOSS CMASS, LOWZ samples are consistent with halo model predictions
- ❖ The measurements can be used for the analysis of cosmology and galaxy-DM relation (e.g., stellar mass-halo mass relation)